Polymer 49 (2008) 3722–3730

Contents lists available at ScienceDirect

Polymer

journal homepage: www.elsevier.com/locate/polymer

Soluble functional polyacetylenes for optical limiting: Relationship between optical limiting properties and molecular structure

Xinyan Su [a,b], Hongyao Xu [a,b,*], Junyi Yang [c], Naibo Lin [a], Yinglin Song [c]

[a] College of Material Science and Engineering and State Key Laboratory for Modification of Chemical Fibers and Polymer Materials, Donghua University, Shanghai 201620, China
[b] School of Chemistry and Chemical Engineering, Anhui University, Hefei 230039, China
[c] Department of Physics, Suzhou University, Suzhou 215008, China

ARTICLE INFO

Article history:
Received 14 February 2008
Received in revised form 27 May 2008
Accepted 16 June 2008
Available online 18 June 2008

Keywords:
Functional polyacetylene
Optical limiting
Nonlinear optics

ABSTRACT

Four polyacetylenes containing chromophores with different conjugation bridge structure or terminal substituents were designed and prepared by using $[Rh(nbd)Cl]_2$ as catalysts, respectively. Their structures and properties were characterized and evaluated by IR, NMR, UV, TGA, optical limiting and nonlinear optical analyses. All the polymers show high thermal and photo stability and novel optical limiting properties. The functional polyacetylene with stilbene pendant shows better optical limiting property than that with azobenzene chromophore pendant. Their optical limiting mechanisms are mainly originated from reverse saturable absorption of molecules. Their nonlinear optical properties are significantly affected by their molecular structures and the shorter spacer group will be beneficial in increasing the electronic interaction between chromophore pendant and polyacetylene conjugation backbone to result in higher third-order optical nonlinearity.

1. Introduction

With the rapid development of new laser technology, the optical limiting materials for protection of optically sensitive devices and human eyes from laser damage in both civilian and military applications in recent years have received significant attention [1–7]. Among the materials, the π-conjugated NLO polymers are considered to be promising materials, mainly because they offer many advantages such as ultrafast time response, high damage threshold, easy molecular design, and good processability to form optical devices. Polyacetylene (PA), the structurally simplest conjugated polymer with alternating single and double bonds, exhibits good third-order electric susceptibilities ($\chi^{(3)}$) and fast response time (the order of several picoseconds) [8–10]. However, the insolubility and instability of this polymer have limited its practical applications as a functional material. Much attention has been redirected to the polyacetylene derivatives substituted by functional group. These functional group substituted polyacetylenes display liquid crystallinity [11–14], photo- and electro-luminescence [15–19], optical activity (chirality) [20,21], photoconductivity [22], gas permeability [23,24], and optical nonlinearity [25–30]. Recently, we have successfully prepared a group of functional polyacetylenes with large third-order nonlinear optical susceptibilities and novel optical limiting properties by copolymerizing phenylacetylene with 4-ethynyl-4′-(*N*,*N*-diethylamino)azobenzene [4]. However, these copolymerized phenylacetylenes possess poorer film-forming properties and limited chromophoric content. To increase chromophoric content and processability, our group has also prepared a series of azobenzene-containing functional poly(1-alkyne)s with different spacer lengths and terminal alkyloxy chains, and found that the azobenzene pendant endowed polyacetylene with novel optical limiting properties and high thermal stability. Simultaneously, flexible spacer between polyacetylene main chain and azobenzene pendant, and the terminal flexible group on azobenzene pendant still impart polyacetylene good solubility and film-forming properties [5,31–33]. To enhance the application of the π-conjugated NLO polymer materials on optical limiters, it is necessary to further understand the relationship between the optical limiting property and the molecular structures of the materials. In this paper, we designed and synthesized four soluble functional polyacetylenes containing chromophore with different conjugation bridge structure or different substituents (Chart 1), and carefully investigated the effects of molecular structures on optical limiting properties of the resultant polymers and their optical limiting mechanisms.

* Corresponding author. College of Material Science and Engineering and State Key Laboratory for Modification of Chemical Fibers and Polymer Materials, Donghua University, Shanghai 201620, China. Tel.: +86 21 67792874.
E-mail address: hongyaoxu@163.com (H. Xu).

0032-3861/$ – see front matter © 2008 Elsevier Ltd. All rights reserved.
doi:10.1016/j.polymer.2008.06.022

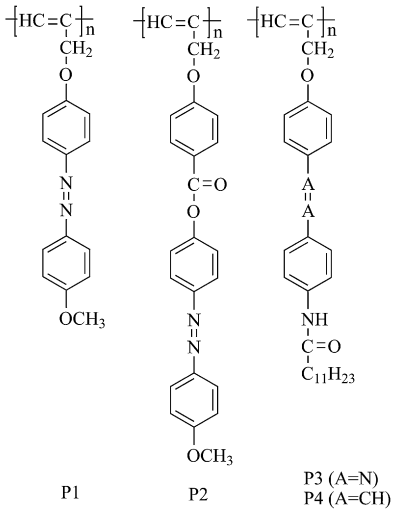

Chart 1.

2. Experimental section

2.1. Materials

Bis(triphenylphosphine)palladium(II) chloride $[Pd(PPh_3)_2Cl_2]$ and norbornadienerhodium(I) chloride dimer $[Rh(nbd)Cl]_2$ were purchased from Aldrich, kept under an inert-atmosphere in a glove box, and used as received without further purification. 4-Methoxyaniline, 4-nitroaniline, 1-(bromomethyl)-4-nitrobenzene, phenol, and propargyl bromide were purchased from Shanghai Chemical Reagent Company. Dioxane, THF, and toluene were distilled from sodium benzophenone ketyl immediately prior to use. Triethylamine was distilled from potassium hydroxide prior to use. Technical grade methanol was used to precipitate the polymers.

2.2. Instruments

The FT-IR spectra were recorded as KBr pellets on a Nicolet 170sx spectrometer. ^{1}H NMR spectra were collected on an AVANCE/DMX-300 MHz Bruker NMR spectrometer. Tetramethylsilane was used as the internal reference for the NMR analyses. Elementary analyses were conducted on Vario EL-III elementary analysis apparatus. UV–vis spectra were recorded on a Shimadzu UV-265 spectrometer using a 1-cm square quartz cell. EI-MS spectra were recorded with a Micromass GCT-MS mass spectrometer. Thermal analyses of the polymers were performed on a Perkin Elmer TGA (Thermogravimetric analysis) under nitrogen at a heating rate of 20 °C/min. Molecular weights of the polymers were estimated by a Waters associates' gel permeation chromatography (GPC) using 12 monodisperse polystyrenes (molecular weight range 10^2–10^7) as calibration standards.

The investigation of the optical limiting properties of the samples was carried out by using a frequency doubled, Q-switched, mode-locked Continuum ns/ps Nd:YAG laser, which provides linearly polarized 4 ns optical pulses at 532 nm wavelength with a repetition of 1 Hz. The experimental arrangement is similar with that in the literature [34]. The samples were housed in quartz cells with a path of 2 mm. The input laser pulses adjusted by an attenuator (Newport) were split into two beams. One was employed as a reference to monitor the incident laser energy, and the other was focused onto the sample cell by using a lens with a 300 mm focal length. The samples were positioned at the focus. The incident and transmitted laser pulses were monitored by two energy detectors, D1 and D2 (Rjp-735 energy probes, Laser Precision).

The nonlinear optical properties of the samples were performed by a Z-scan technique with the same laser system as in the optical limiting experiment with a pulse width of 4 ns at 1 Hz repetition rate and 532 nm wavelengths. The experiment was set up as in the literature [35]. The solution sample was contained in a 2 mm quartz cell. The input energy was 40 μJ. The radius ω_0 at beam waist was 70 mm. The samples were moved along the axis of the incident beam (z direction). The experimental data were collected utilizing a single shot at a rate of 1 pulse/min to avoid the influence of thermal effect.

2.3. Monomer synthesis

2.3.1. Synthesis of 4-((4-methoxyphenyl)diazenyl)phenol (**1a**)

4-Methoxyaniline (9.85 g, 0.08 mol) was dissolved in 32 mL conc. hydrochloric acid. After cooling to 0 °C, an ice-water solution of 5.52 g (0.08 mol) sodium nitrite was added dropwise and stirred for 30 min. Phenol (7.88 g, 0.084 mol) was dissolved in 60 mL aqueous NaOH (3.36 g, 0.084 mol) solution. Then this solution was added to 2 L aqueous buffer solution of NH_4Cl–$NH_3\cdot H_2O$ (pH ≈ 9). The so-formed diazonium chloride solution was added to the buffer solution and stirred for 2 h at 0–5 °C. The mixture was adjusted to pH ≈ 6 using aqueous HCl solution and the resulting precipitate was filtered, rinsed with water twice. The crude product was recrystallized from ethanol twice to give dark red piece crystals in 85% yield. FT-IR (KBr), ν (cm^{-1}): 3418 (OH), 2918, 2843 (CH_3), 1588, 1508, 1458 (CH═CH), 1238 (C–O–C). ^{1}H NMR (300 MHz, $CDCl_3$): δ 3.88 (s, 3H, CH_3), 5.24 (s, 1H, OH), 6.93 (d, 2H, $J = 8.8$ Hz, H^7), 6.99 (d, 2H, $J = 9.0$ Hz, H^2), 7.83 (d, 2H, $J = 8.8$ Hz, H^6), 7.87 (d, 2H, $J = 9.0$ Hz, H^3). Anal. Calcd for $C_{13}H_{12}N_2O_2$: C 68.41, H 5.30, N 12.27. Found: C 68.37, H 5.26, N 12.34.

2.3.2. Synthesis of 4-((4-nitrophenyl)diazenyl)phenol (**1b**)

This was prepared as above from 4-nitroaniline. The crude product was recrystallized from ethanol twice to give orange crystals in 87% yield. FT-IR (KBr), ν (cm^{-1}): 3416 (OH), 1593, 1508, 1458 (Ar), 1335 (NO_2). ^{1}H NMR (300 MHz, $CDCl_3$): δ 5.34 (s, 1H, OH), 6.98 (d, 2H, $J = 8.5$ Hz, H^7); 7.94 (d, 2H, $J = 8.5$ Hz, H^6), 7.83 (d, 2H, $J = 8.7$ Hz, H^3), 7.87 (d, 2H, $J = 8.7$ Hz, H^2). Anal. Calcd for $C_{12}H_9N_3O_3$: C 59.26, H 3.73, N 17.28. Found: C 59.17, H 3.70, N 17.32.

2.3.3. Synthesis of 1-(4-methoxyphenyl)-2-(4-(prop-2-ynyloxy)phenyl)diazene (**M1**)

Sodium hydroxide (0.8 g, 0.02 mol) was added to a solution of 4.56 g (0.02 mol) **1a** in 50 mL ethanol. After the reaction mixture was stirred at room temperature for 1 h, 3.57 g (0.03 mol) propargyl bromide was added dropwise to the mixture. The resulting mixture was heated under reflux overnight. Ether was added to the mixture, and the organic phase was washed with water. The organic phase was dried over $MgSO_4$. After the removal of the solvent with a rotary evaporator, the residue was recrystallized from ethanol twice to give orange piece crystals in 84% yield. FT-IR (KBr), ν (cm^{-1}): 3276 (≡C–H), 3053 (═C–H), 2912, 2840 (CH_3, CH_2), 2129 (C≡C), 1596, 1500, 1465 (CH═CH), 1251 (C–O–C), 844 (*p*-Ar). ^{1}H NMR (300 MHz, $CDCl_3$): δ 2.58 (t, 1H, $J = 2.4$ Hz, ≡CH), 3.91 (s, 3H, CH_3), 4.79 (d, 2H, $J = 2.4$ Hz, OCH_2), 7.02 (d, 2H, $J = 8.8$ Hz, H^7), 7.10 (d, 2H, $J = 8.8$ Hz, H^2), 7.90 (d, 4H, $J = 8.8$ Hz, $H^{3,6}$). ^{13}C NMR (75 MHz, $CDCl_3$): δ 161.2 (C^8), 158.9 (C^1), 147.2 (C^5), 146.6 (C^4), 123.9 (C^6), 114.6 (C^7), 113.7 (C^2), 76.7 (*C*≡), 75.4 (≡CH), 55.5 (OCH_2), 55.1 (OCH_3). Anal. Calcd for $C_{16}H_{14}N_2O_2$: C 72.16, H 5.30, N 10.52. Found: C 72.13, H 5.23, N 10.57. MS (EI), m/z [M^+]: 266.1057, calcd: 266.1055.

2.3.4. Synthesis of 1-(4-nitrophenyl)-2-(4-(prop-2-ynyloxy)-phenyl)diazene (**2b**)

This was prepared as above from **1b**. The crude product was recrystallized from ethanol twice to give brown piece crystals in

87% yield. FT-IR (KBr), ν (cm^{-1}): 3263 (≡C–H), 2919, 2862 (CH_2), 2125 (C≡C), 1589, 1500 (C═C), 836 (*p*-Ar). ^1H NMR (300 MHz, $CDCl_3$): δ 2.58 (t, 1H, $J = 2.4$ Hz, ≡C*H*), 4.81 (d, 2H, $J = 2.4$ Hz, OCH_2), 7.13 (d, 2H, $J = 8.7$ Hz, H^7), 7.99 (d, 4H, $J = 8.7$ Hz, $H^{3,6}$), 7.90 (d, 2H, $J = 8.7$ Hz, H^2). Anal. Calcd for $C_{15}H_{11}N_3O_3$: C 64.05, H 3.94, N 14.94. Found: C 63.98, H 3.91, N 15.01.

2.3.5. Synthesis of 4-(prop-2-ynyloxy)benzoic acid (**2c**)

The procedure was similar to the above from 4-hydroxybenzoic acid. After cooling to room temperature, 1 mol/L HCl solution was added to neutralize the reaction mixture. The white precipitate was filtered and recrystallized from ethanol twice to give white piece crystals in 75% yield. FT-IR (KBr), ν (cm^{-1}): 3267 (≡C–H), 2972, 2852 (CH_2), 2130 (C≡C), 1689 (C═O), 1593 (Ar), 1249 (C–O–C). ^1H NMR (300 MHz, $CDCl_3$): δ 2.54 (t, 1H,≡C*H*), 4.78 (d, 2H, OCH_2), 7.09 (d, 2H, $J = 8.4$ Hz, H^{11}), 8.07 (d, 2H, H^{12}). Anal. Calcd for $C_{10}H_8O_3$: C 68.18, H 4.58. Found: C 68.12, H 4.61.

2.3.6. Synthesis of 4-(prop-2-ynyloxy)benzaldehyde (**2d**)

This was prepared as above from 4-hydroxy benzaldehyde and potassium carbonate was used as base. The crude product was purified by silica gel column chromatography (eluent: petroleum ether/ethyl acetate = 4/1, volume ratio) to obtain white crystal in 83% yield. FT-IR (KBr), ν (cm^{-1}): 3209 (≡C–H), 2836 (CH_2), 2756 (CHO), 2120 (C≡C), 1682 (C═O), 1604 (Ar), 1247 (C–O–C), 836 (*p*-Ar). ^1H NMR (300 MHz, $CDCl_3$): δ 2.59 (s, 1H, ≡C*H*), 4.80 (s, 2H, OCH_2), 7.10 (d, 2H, $J = 8.4$ Hz, H^7), 7.87 (d, 2H, H^6), 9.92 (s, 1H, C*H*O). Anal. Calcd for $C_{10}H_8O_2$: C 74.99, H 5.03. Found: C 74.81, H 4.99.

2.3.7. Synthesis of 1-nitro-4-(4-(prop-2-ynyloxy)styryl)-benzene (**3d**)

This was prepared from 4-(prop-2-ynyloxy)benzaldehyde and 1-(bromomethyl)-4-nitrobenzene by Wittig reaction according to the literature [36]. The crude product was purified by silica gel column chromatography (eluent: petroleum ether/ethyl acetate = 3/1, volume ratio) to obtain yellow crystals in 70% yield. FT-IR (KBr), ν (cm^{-1}): 3263 (≡C–H), 2921, 2867 (CH_2), 2125 (C≡C), 1589, 1500 (C═C), 1334 (NO_2), 836 (*p*-Ar). ^1H NMR (300 MHz, $CDCl_3$): δ 2.53 (s, 1H, ≡C*H*), 4.72 (s, 2H, OCH_2), 7.01 (d, 2H, $J = 8.7$ Hz, H^7), 7.07 (d, 2H, $J = 15.6$ Hz, ═C*H*), 7.50 (d, 2H, $J = 8.7$ Hz, H^3), 7.59 (d, 2H, $J = 8.7$ Hz, H^6), 8.20 (d, 2H, $J = 8.7$ Hz, H^2). Anal. Calcd for $C_{17}H_{13}NO_3$: C 73.11, H 4.69, N 5.02. Found: C 73.07, H 4.71, N 5.06.

2.3.8. Synthesis of 4-((4-(prop-2-ynyloxy)phenyl)-diazenyl)benzenamine (**3b**)

Compound **2b** (2.81 g, 0.01 mol) was added to a 250 mL flask with 120 mL ethanol, a solution of cooled stannous chloride 11.3 g (0.05 mol) in conc. hydrochloric acid (30 mL) was added dropwise to the resulting solution and stirred. Then the solution was refluxed for 8 h, after cooling to room temperature, 1 M NaOH solution was added to neutralize the reaction mixture and the resulting precipitate was filtered. Then the precipitate was dissolved in toluene, and the insoluble part was removed by filtration. The toluene solution was dried over $MgSO_4$. After the removal of the solvent with a rotary evaporator, the residue was recrystallized from ethanol twice to give brown solid in 62% yield. FT-IR (KBr), ν (cm^{-1}): 3486, 3388 (NH_2), 3268 (≡C–H), 2913, 2860 (CH_2), 2125 (C≡C), 1596, 1506 (C═C), 831 (*p*-Ar). ^1H NMR (300 MHz, $CDCl_3$): δ 2.56 (s, 1H, ≡C*H*), 4.01 (br, 2H, NH_2), 4.76 (s, 2H, OCH_2), 6.73 (d, 2H, $J = 8.8$ Hz, H^2), 7.07 (d, 2H, $J = 8.8$ Hz, H^7), 7.77 (d, 2H, $J = 8.8$ Hz, H^3), 7.85 (d, 2H, $J = 8.7$ Hz, H^6). Anal. Calcd for $C_{15}H_{13}N_3O$: C 71.70, H 5.21, N 16.72. Found: C 71.62, H 5.17, N 16.76.

2.3.9. Synthesis of 4-(4-(prop-2-ynyloxy)styryl)benzenamine (**4d**)

This was prepared as above from **3d**. The crude product was recrystallized from ethanol twice to give pale brown powder in 58% yield. FT-IR (KBr), ν (cm^{-1}): 3410, 3380 (NH_2), 3282 (≡C–H), 2867 (CH_2), 2124 (C≡C), 1606, 1512 (C═C), 829 (*p*-Ar). ^1H NMR (300 MHz, $CDCl_3$): δ 2.52 (s, 1H, ≡C*H*), 4.70 (s, 2H, OCH_2), 6.67 (d, 2H, $J = 8.4$ Hz, H^2), 6.86 (d, 2H, $J = 16.2$ Hz, ═C*H*), 6.95 (d, 2H, $J = 8.4$ Hz, H^7), 7.31 (d, 2H, $J = 8.7$ Hz, H^3), 7.42 (d, 2H, $J = 8.7$ Hz, H^6). Anal. Calcd for $C_{17}H_{15}NO$: C 81.90, H 6.06, N 5.62. Found: C 81.82, H 6.07, N 5.66.

2.3.10. Synthesis of 4-((4-methoxyphenyl)diazenyl)phenyl 4-(prop-2-ynyloxy)benzoate (**M2**)

In a two-necked, 250-mL, round-bottom flask under nitrogen were added 3.52 g (0.02 mol) of **2c** and 2 mL of $SOCl_2$ in 60 mL of anhydrous toluene. The mixture was refluxed at 80 °C for 5 h. The solvent and excessive $SOCl_2$ were removed under reduced pressure, and the residue was dissolved in 40 mL anhydrous THF with 3 mL anhydrous Et_3N. The solution was cooled to 0 °C, and then 5.01 g (0.022 mol) **1a** was added. After 12 h of refluxing, the solvent was removed under reduced pressure, and the crude product was purified by Al_2O_3 column chromatography with a mixture of ethyl acetate and petroleum ether (1:4 v/v) as the eluent. After further purification by recrystallization from anhydrous ethanol, monomer **M2** was obtained as orange crystals in 80% yield. FT-IR (KBr) cm^{-1}: 3246 (≡C–H), 2918, 2840 (CH_3), 2129 (C≡C), 1719 (C═O), 1602, 1580, 1503 (Ar), 1255 (C–O–C), 840 (*p*-Ar). ^1H NMR (300 MHz, $CDCl_3$): δ 2.58 (t, 1H, $J = 2.4$ Hz, ≡C*H*), 3.89 (s, 3H, CH_3), 4.80 (d, 2H, $J = 2.4$ Hz, OCH_2), 7.02 (d, 2H, $J = 9.2$ Hz, H^2), 7.09 (d, 2H, $J = 9.2$ Hz, H^3), 7.35 (d, 2H, $J = 8.8$ Hz, H^{11}), 7.93 (d, 2H, $J = 8.8$ Hz, H^7), 7.96 (d, 2H, $J = 8.8$ Hz, H^6), 8.20 (2H, d, $J = 8.8$ Hz, H^{10}). ^{13}C NMR(75 MHz, $CDCl_3$): δ 163.9 (*C*═O), 161.6 (C12), 161.3 (C1), 152.1 (C8), 149.9 (C5), 146.5 (C4), 131.8 (C10), 124.3 (C3), 123.3 (C6), 122.0 (C9), 121.8 (C7), 114.3 (C2), 113.7 (C11), 76.7 (*C*≡), 75.7 (≡CH), 55.4 (OCH_2), 55.1 (OCH_3). Anal. Calcd for $C_{23}H_{18}N_2O_4$: C 71.49, H 4.70, N 7.25. Found: C 71.42, H 4.68, N 7.31. MS (EI), *m*/*z* [M^+]: 386.1265, calcd: 386.1267.

2.3.11. Synthesis of N-(4-((4-(prop-2-ynyloxy)phenyl)diazenyl)-phenyl)dodecanamide (**M3**)

This was prepared as above from dodecanoic acid and **3b**. The crude product was purified by Al_2O_3 column chromatography with a mixture of ethyl acetate and petroleum ether (1:4 v/v) as the eluent. After further purification by recrystallization from anhydrous ethanol, monomer **M3** was obtained as brown solid in 83% yield. FT-IR (KBr) cm^{-1}: 3290 (≡C–H), 3050 (═C–H), 2920, 2850 (CH_3, CH_2), 2133 (C≡C), 1663 (C═O), 1599, 1536, 1500 (CH═CH), 1247 (C–O–C), 846 (*p*-Ar). ^1H NMR (300 MHz, $CDCl_3$): δ 0.88 (CH_3), 1.26 (br, 16H, $CH_3(CH_2)_8$), 1.74 (m, 2H, CH_2CH_2CONH), 2.39 (t, 2H, CH_2CONH), 2.56 (t, 1H, $J = 2.4$ Hz, ≡C*H*), 4.77 (d, 2H, $J = 2.4$ Hz, OCH_2), 7.08 (d, 2H, $J = 9.2$ Hz, H^7), 7.30 (br, 1H, CON*H*), 7.67 (d, 2H, $J = 8.4$ Hz, H^2), 7.90 (t, 4H, $H^{3,6}$). ^{13}C NMR (75 MHz, $CDCl_3$): δ 171.5 (*C*═O), 159.7 (C8), 149.1 (C4), 147.6 (C5), 140.1 (C1), 124.5 (C6), 123.7 (C3), 119.7 (C2), 115.2 (C7), 78.1 (≡*C*), 75.9 (≡CH), 56.0 (OCH_2), 37.9 (CH_2CONH), 31.9 ($CH_3CH_2CH_2$), 29.7–29.3 [$C_3H_7(CH_2)_6$], 25.5 (CH_2CH_2CONH), 22.5 (CH_3CH_2), 14.1 (CH_3). Anal. Calcd for $C_{27}H_{35}N_3O_2$: C 74.79, H 8.14, N 9.69. Found: C 71.62, H 8.19, N 9.73. MS (EI), *m*/*z* [M^+]: 433.2727, calcd: 433.2729.

2.3.12. Synthesis of N-(4-(4-(prop-2-ynyloxy)styryl)phenyl)-dodecanamide (**M4**)

This was prepared as above from dodecanoic acid and **4d**. The crude product was purified by Al_2O_3 column chromatography with a mixture of ethyl acetate and petroleum ether (1:4 v/v) as the eluent. After further purification by recrystallization from anhydrous ethanol, monomer **M4** was obtained as pale brown crystals in 77% yield. FT-IR (KBr), ν (cm^{-1}): 3291 (≡C–H), 3050 (═C–H), 2920, 2851 (CH_3, CH_2), 2134 (C≡C), 1665 (C═O), 1599, 1536, 1500 (CH═CH), 1247 (C–O–C), 846 (*p*-Ar).^1H NMR (300 MHz, $CDCl_3$): δ 0.90 (CH_3), 1.28 (br, 16H, $CH_3(CH_2)_8$), 1.75 (m, 2H, CH_2CH_2CONH),

2.38 (t, 2H, CH_2CONH), 2.56 (t, 1H, $J = 2.4$ Hz, ≡CH), 4.74 (d, 2H, $J = 2.4$ Hz, OCH_2), 6.95 (d, 1H, $J = 16.4$ Hz, =CH), 6.99 (d, 2H, $J = 8.8$ Hz, H^7), 7.04 (d, 1H, $J = 16.4$ Hz, =CH), 7.14 (br, 1H, CONH), 7.47 (t, 4H, $H^{3,6}$), 7.53 (d, 2H, $J = 8.8$ Hz, H^2). ^{13}C NMR (75 MHz, $CDCl_3$): δ 171.1 (C=O), 157.5 (C8), 137.1 (C1), 130.6 (C4), 127.6 (C6, CH=CH), 127.2 (C5), 126.9 (C3), 119.8 (C2), 115.2 (C7), 78.3 (≡C), 75.6 (≡CH), 55.9 (OCH_2), 34.3 (CH_2CONH), 31.9 ($CH_3CH_2CH_2$), 29.1–29.6 [$C_3H_7(CH_2)_6$], 25.6 (CH_2CH_2CONH), 22.7 (CH_3CH_2), 14.1 (CH_3). Anal. Calcd for $C_{29}H_{37}NO_2$: C 80.70, H 8.64, N 3.25. Found: C 80.61, H 8.58, N 3.27. MS (EI), m/z [M^+]: 431.2829, calcd: 431.2824.

2.4. Polymerization

All the polymerization reactions and manipulations were performed under pre-purifed nitrogen using Schlenk techniques either in vacuum-line system of an inert-atmosphere glove box, except for the purification of the polymers, which were done in open air. Typical procedures for the polymerization are given below: Into a baked 20-mL Schlenk tube with a side arm was added 1 mmol of the monomer. The tube was evacuated under vacuum and then flushed with dry nitrogen three times through the side arm. Dioxane (3 mL) was injected into the tube to dissolve the monomer. The catalyst solution was prepared in another tube by dissolving 4.6 mg (0.01 mmol) $[Rh(nbd)Cl]_2$ and 2.02 mg (0.02 mmol) Et_3N in 2 mL of dioxane, which was transferred to the monomer solution using a hypodermic syringe. The reaction mixture was stirred at 60 °C under nitrogen for 6 h. The mixture was then diluted with 5 mL of dioxane and added dropwise to 200 mL of methanol under stirring. The precipitate was centrifuged and redissolved in THF. The THF solution was added dropwise into 200 mL of methanol to precipitate the polymer. The dissolution–precipitation process was repeated three times, and the finally isolated precipitant was dried under vacuum at 30 °C to a constant weight.

2.4.1. Characterization data

P1: Deep brown solid; yield 61.3%, $M_w = 1.27 \times 10^4$, $M_w/M_n = 2.5$ (GPC, Table 1, no.1). FT-IR (KBr) cm^{-1}: 3053 (=C–H), 2912, 2840 (CH_3, CH_2), 1596, 1500, 1465 (CH=CH), 1251 (C–O–C), 844 (*p*-Ar). ^{1}H NMR (300 MHz, $CDCl_3$): δ 3.90 (br, CH_3), 5.22 (br, =CCH_2O), 7.01, 7.91 (br, *trans* =C–H and Ar–H).

P2: Deep brown solid; yield 58.7%, $M_w = 1.75 \times 10^4$, $M_w/M_n = 1.8$ (GPC, Table 1, no.2). FT-IR (KBr) cm^{-1}: 3073 (=CH), 2925, 2841 (CH_3, CH_2), 1732 (C=O), 1601 (CH=CH), 1253 (C–O–C), 840 (*p*-Ar). ^{1}H NMR (300 MHz, $CDCl_3$): δ 3.90 (br, CH_3), 5.23 (br, =CCH_2O), 7.00, 7.32, 7.91, 8.17 (br, *trans* =C–H and Ar–H).

P3: Deep brown solid; yield 66.9%, $M_w = 1.51 \times 10^4$, $M_w/M_n = 2.2$ (GPC, Table 1, no.3). FT-IR (KBr) cm^{-1}: 3305 (NH), 3050 (=CH), 2923, 2851 (CH_3, CH_2), 1667 (C=O), 1597 (CH=CH), 1241 (C–O–C), 843 (*p*-Ar). ^{1}H NMR (300 MHz, $CDCl_3$): δ 0.87 (CH_3), 1.25 (br, 16H, $CH_3(CH_2)_8$), 1.74 (m, 2H, CH_2CH_2CONH), 2.40 (t, 2H, CH_2CONH), 4.99 (br, 2H, OCH_2), 6.95 (br, Ar–H and *trans* =C–H), 7.30 (br, 1H, CONH), 7.62–7.90 (br, Ar–H).

P4: Brown solid, yield 60.2%, $M_w = 1.34 \times 10^4$, $M_w/M_n = 1.2$ (GPC, Table 1, no.10). FT-IR (KBr) cm^{-1}: 3304 (NH), 3049 (=CH), 2921, 2851 (CH_3, CH_2), 1667 (C=O), 1597 (CH=CH), 1241 (C–O–C), 843 (*p*-Ar). ^{1}H NMR (300 MHz, $CDCl_3$): δ 0.90 (CH_3), 1.27 (br, 16H, $CH_3(CH_2)_8$), 1.76 (m, 2H, CH_2CH_2CONH), 2.38 (t, 2H, CH_2CONH), 5.14 (br, 2H, OCH_2), 6.93 (br, Ar–H and *trans* =C–H), 7.15 (br, 1H, CONH), 7.45, 7.54 (br, Ar–H).

Table 1
Polymerization of four 1-alkynes[a]

No.	Monomer	Temperature (°C)	Time (h)	Yield (%)	M_w[b]	M_w/M_n[b]
1	**M1**	60	6	61.3	12,700	2.5
2	**M2**	60	6	58.7	17,500	1.8
3	**M3**	60	6	66.9	15,100	2.2
4	**M3**	60	3	55.1	9800	1.4
5	**M3**	60	12	68.2	10,500	1.3
6	**M3**	30	3	47.5	5850	1.4
7	**M3**	90	3	65.4	10,300	1.6
8[c]	**M3**	60	6	70.5	10,200	1.3
9[d]	**M3**	60	6	63.1	11,300	2.7
10	**M4**	60	6	60.2	13,400	1.4

[a] Unless otherwise specified, the polymerization was carried out in dioxane under nitrogen with $[Rh(nbd)Cl]_2$–Et_3N as a catalyst.
[b] Estimated by GPC on the basis of polystyrene calibration.
[c] In THF.
[d] In toluene.

3. Results and discussion

3.1. Monomer synthesis

We prepared four monosbstistuted acetylene monomers containing different chromophore pendants or terminal substituents through a multi-step synthesis route (Scheme 1) in high yeild. The diazotization-coupling reaction of aniline derivatives with phenol gave azobenzene derivatives **1a** and **1b**. Then, **1a**, **1b**, and 4-hydroxybenzoic acid, as well as 4-hydroxy benzaldehyde were etherized with propargyl bromide to give compounds **M1**, **2b**, **2c**, and **2d**, respectively. Compound **3d** was prepared by Wittig reaction from **2d** and 1-(bromomethyl)-4-nitrobenzene. Compounds **2b** and **3d** were reduced with stannous chloride dehydrate in conc. HCl to give **3b** and **4d**. Treatment of **2c** with thionyl chloride, followed by a reaction with **1a** yielded the desirable monomer **M2**. **M3** and **M4** are prepared in a similar way from dodecanoic acid and corresponding amine (**3b** or **4d**).

3.2. Polymerization reactions

All polymerization reactions were carried out under nitrogen atmosphere using a standard Schlenk vacuum-line system. Because monomers contained polar azo groups, metathesis catalysts such as WCl_6 and $MoCl_5$ failed to initiate the polymerizations. On the contrary, $[Rh(nbd)Cl]_2/Et_3N$ catalyst [37] effectively worked for the polymerization and the results are listed in Table 1. The reaction of **M1** in dioxane at 60 °C for 6 h produced a deep brown product in a yield of 61.3% with an M_w value of 12,700 (Table 1, no. 1). Under the same conditions, **M2**, **M3** and **M4** can be effectively polymerized to yield resultant polymers in moderate yields. To optimize the polymerization process, we studied the polymerizations of **M3** under different reaction conditions. Prolonging or shortening the reaction time to 12 or 3 h hardly improved the results. Raising the temperature to 90 °C, the yield and the molecular weight of the resulting polymer changed slightly. When the polymerization was carried out at 30 °C, both the yield and the M_w value decreased significantly. The polymerization also works in THF and toluene, but the molecular weight became lower (Table 1, nos. 8 and 9).

3.3. Structural characterization

All the purified polymerization products gave satisfactory spectroscopic data corresponding to their expected molecular structures. Typical example of the IR spectra of polymer **P3** and monomer **M3** is shown in Fig. 1. As can be seen from Fig. 1, **M3** clearly shows characteristic C≡H and C≡C stretching vibrations at 3290 and 2133 cm^{-1}, respectively. The aromatic rings exhibit a weak =CH stretching band at 3050 cm^{-1}, and the C=O in **M3** absorbs strongly at 1663 cm^{-1}. However, all the acetylenic absorption bands disappear in the spectrum of polymer **P3** (Table 1, no. 3), and the relative intensity of the stretching band at 3050 cm^{-1} (vs CH_3, CH_2 absorption band at 2923, 2851 cm^{-1}) and

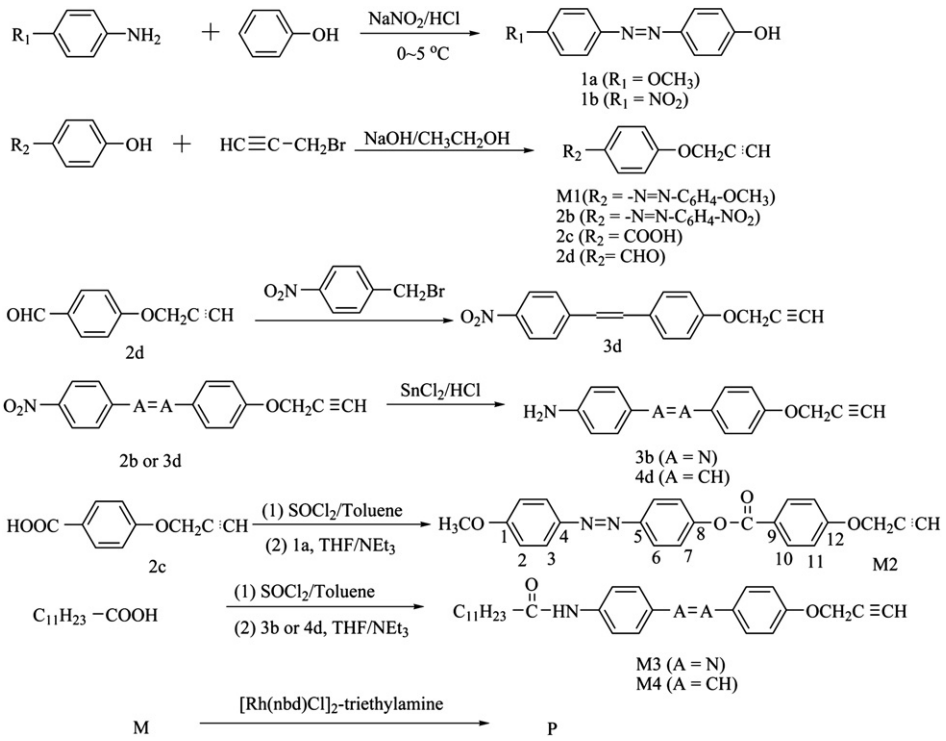

Scheme 1. Synthesis route.

1597 cm^{-1} (vs C═O absorption band at 1667 cm^{-1}) increased, suggesting that the resulting polymer possesses a polyacetylene molecular structure and confirming that Rh catalyst has initiated the acetylene polymerization.

Fig. 2 shows ^{1}H NMR spectra of polymer **P3** (Table 1, no. 3) and monomer **M3.** The signal at 2.56 ppm in the ^{1}H NMR spectrum of monomer **M3** assigned to the acetylenic proton was not observed in the ^{1}H NMR spectrum of its relative polymer **P3.** However, a broad peak at δ 6.95 ppm corresponding to the olefin protons and aromatic protons absorption, hint that acetylene triple bonds (C≡C) of monomer **M3** have been converted to the polyene double bonds (C═C) of the polymers by the acetylene polymerization. Simultaneously, the absorption of the propargyl proton in the ^{1}H NMR spectrum of the polymer became broader due to its transformation to the allylic structure [33], further confirming that the triple bonds of the monomers have been converted to polymer main chains composing of alternating single-double bonds. Similar results were found in spectra of other polymers.

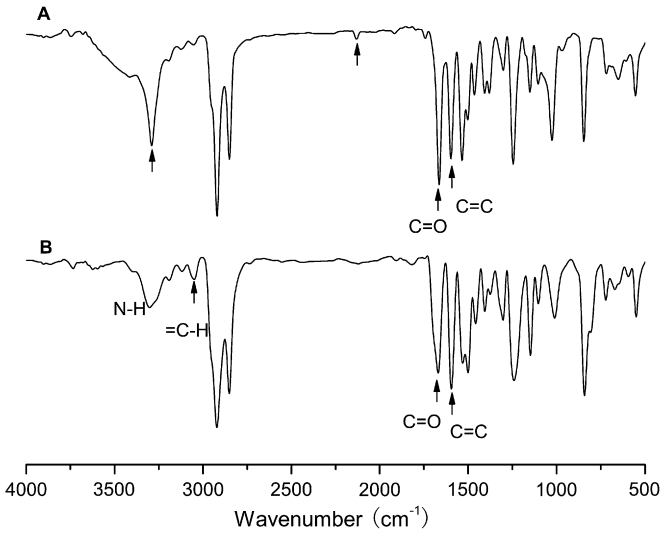

Fig. 1. IR spectra of (A) **M3** and (B) its polymer **P3** (sample from Table 1, no. 3).

3.4. Linear optical properties

The UV spectra of the polymers in THF are depicted in Fig. 3. As shown in Fig. 3, polymers **P1**–**P3** show strong absorption peaks located at 358, 350, and 366 nm, respectively, which are assigned to π–π^* electronic transitions of the pedant azobenzene groups. The

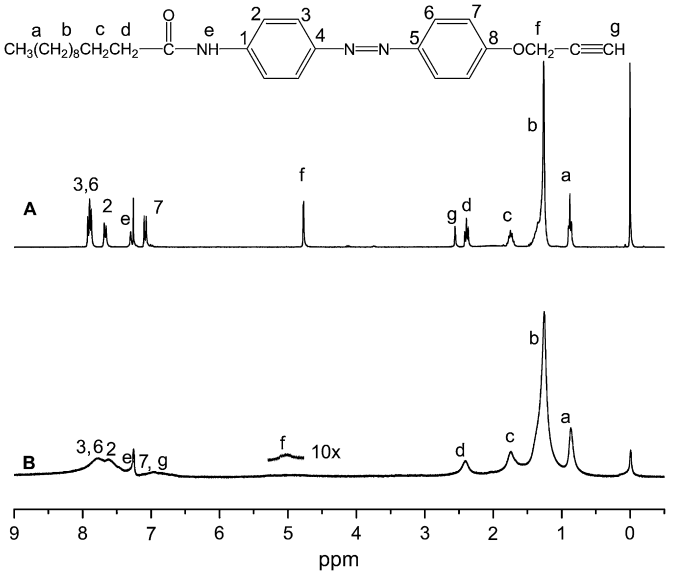

Fig. 2. ^{1}H NMR spectra of (A) **M3** and (B) its polymer **P3** (Table 1, no. 3) in chloroform-*d*.

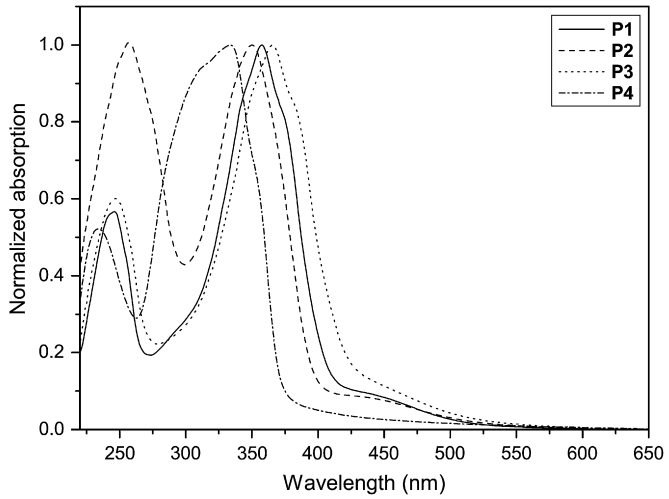

Fig. 3. Normalized linear absorption spectra of **P1** (Table 1, no. 1), **P2** (Table 1, no. 2), **P3** (Table 1, no. 3), and **P4** (Table 1, no. 10) in THF.

maximum absorption peak of **P2** in the UV spectra showed 8 nm blue shifts compared with that of **P1**, which may result from the rigid spacer –PhCOO– group twisting the planar azobenzene group. When methoxyl group was replaced with amido group, the maximum absorption peak of **P3** shows 8 nm red shifts in comparison with that of **P1**, which may be due to a more regular arrangement of the molecules induced by the hydrogen band between amido groups that existed in **P3**, which have been confirmed in our previous work [38]. In addition, **P4** displayed the maximum absorption peak at 334 nm and 32 nm blue shifts relative to **P3** due to different π conjugation bridge structure. The backbone absorptions were found at wavelength 400 nm with low intensities.

3.5. Thermal analysis of polymers

The thermal stability of the resulting polymers was evaluated by themogravimeric analysis (TGA) under nitrogen atmosphere. Their TGA thermograms are shown in Fig. 4. It is known that poly(1-alkyne)s such as poly(1-butyne) and poly(1-hexyne), are so unstable that even the isolation process of the polymer products from the polymerization reactions leads to degradation and poly(1-hexyne) starts to lose its weight at 150 °C, and heating for a few minutes at the temperature easily changes the yellow powder to a brown gummy fluid [39–41]. However, except for the polymerization reactions in our preparation, which were carried out under an atmosphere of dry nitrogen, all the handlings including the isolation, purification, and storage of all the polymers were done in an open atmosphere, during which no any changes in the color and form of the polymer products were observed. On the other hand, as shown in Fig. 4, the decomposition temperatures T_ds (defined as the temperature of 5% weight loss) were 222, 238, 267 and 281 °C for **P1**–**P4**, respectively. Thus, the incorporation of the rigid azobenzene or stilbene group into poly(1-alkyne)s endowed the polymers with high thermal stability. The enhanced thermal stability of these polymers may have been originated from the "jacket effect" of the aromatic azobenzene or stilbene pendants [42]. Similar results were also found by Masuda, Tang and our group [33,37,43].

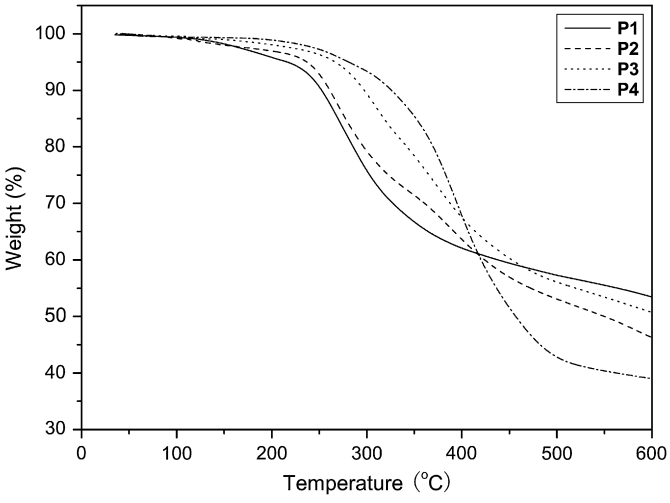

Fig. 4. TGA thermograms of polymers **P1** (sample from Table 1, no. 1), **P2** (Table 1, no. 2), **P3** (Table 1, no. 3), and **P4** (Table 1, no. 10) recorded under nitrogen at a heating rate of 20 °C/min.

3.6. Nonlinear optical property

The nonlinear absorption coefficients of the polymers are measured by Z-scan technique. The results of Z-scan with and without an aperture show that polymers **P1**–**P3** have both nonlinear absorption and refraction, while polymer **P4** only has nonlinear absorption. The Z-scan results of **P3** are shown exemplarily in Fig. 5.

In theory, the normalized transmittance for the open aperture configuration can be written as [33,35]

$$T(z, s = 1) = \sum_{m=0}^{\infty} \frac{[-q_0(z)]^m}{(m+1)^{3/2}}, \quad \text{for } |q_0| < 1 \tag{1}$$

where $q_0(z) = \alpha_2 I_0(t) L_{\text{eff}}/(1 + z^2/z_0^2)$, α_2 is the nonlinear absorption coefficient, $I_0(t)$ the intensity of laser beam at focus ($z = 0$), $L_{\text{eff}} = [1 - \exp(-\alpha_0 L)]/\alpha_0$ is the effective thickness with α_0 the linear absorption coefficient and L the sample thickness, z_0 is the diffraction length of the beam, and z is the sample position. Thus, the nonlinear absorption coefficient of the polymers can be determined by fitting the experimental data using Eq. (1).

The normalized transmission for the closed aperture Z-scan is given by [33,35]

$$T(z, \Delta\phi) = 1 + \frac{4\Delta\phi x}{(x^2+9)(x^2+1)} \tag{2}$$

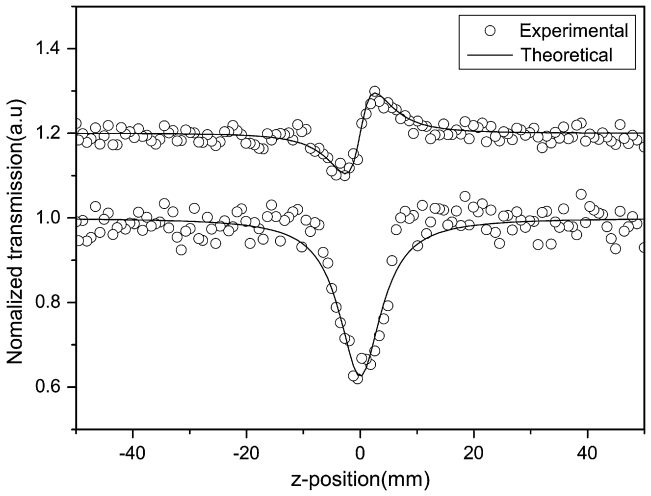

Fig. 5. Z-scan data of **P3** (sample taken from Table 1, no. 3) in THF.

where $x = z/z_0$ and $\Delta\phi$ is on-axis phase change caused by the nonlinear refractive index of the sample and $\Delta\phi = 2\pi I_0(1 - e^{-\alpha_0 L})n_2/\lambda\alpha_0$. Thus, the nonlinear refractive coefficient of the polymers can be determined by fitting the experimental data using Eq. (2).

The $\chi^{(3)}$ can be calculated by the following equation [33,35]

$$\left|\chi^{(3)}\right| = \sqrt{\left|\frac{cn_0^2}{80\pi}\cdot n_2\right|^2 + \left|\frac{9\times 10^8 \varepsilon_0 n_0^2 c^2}{4\pi\omega}\cdot \alpha_2\right|^2} \quad (3)$$

where ε_0 is the permittivity of vacuum, c the speed of light, n_0 the refractive index of the medium and $\omega = 2\pi c/\lambda$. The calculation results of the nonlinear optical coefficients for the four polymers are shown in Table 2. From Table 2, it can be seen that the nonlinear susceptibilities $\chi^{(3)}$ of **P1**–**P4** are 2.28×10^{-11}, 2.24×10^{-11}, 1.69×10^{-11} and 4.69×10^{-12} esu, respectively, which are almost 1–2 orders of magnitude larger than those of poly(phenylacetylene) [30,44,45], and larger than poly(*N*-carbazolylacetylene) [30], poly(1-naphthylacetylene) [30], and as well as poly(EAAB-*co*-PA) [4] and azobenzene-containing substituted poly(1-alkyne)s [46]. Based on the Schweig's nonlinear optical theory of the relationship between molecular structure and optical property, the large optical nonlinearities of these polymers may be attributed to the electronic interaction of the large second-order nonlinear optical chromophore (azobenzene or stilbene) and the conjugative polyacetylene main chain. Simultaneously, it is also found from Table 2 that **P1** shows slightly larger $\chi^{(3)}$ value than **P2**, which may result from the decrease of the electronic interactions of azobenzene with polyacetylene main chain due to the existence of the longer spacer –PhCOO– group. The longer flexible imide group as terminal group significantly lowers the $\chi^{(3)}$ value of resultant polymer. The third-order nonlinear optical susceptibility of the polymers is significantly affected by π-bridge structure. **P3** with chromophore group of N=N double bond as conjugation bridge shows larger third-order nonlinearity than that of **P4** with C=C as π-conjugation bridge structure. Similar results are also found by Xu et al. [47].

3.7. Optical limiting properties

Fig. 6 shows the optical limiting behaviors of **P1** (Table 1, no. 1, $c = 0.42$ mg/mL), **P2** (Table 1, no. 2, $c = 0.45$ mg/mL), **P3** (Table 1, no. 3, $c = 0.35$ mg/mL), and **P4** (Table 1, no. 10, $c = 0.52$ mg/mL) at the same linear transmittance ($T = 71\%$) in THF and the results are also summarized in Table 2. As shown in Fig. 6, at very low incident fluence, the output fluence of all the polymer solutions increases linearly with the incident fluence obeying the Beer–Lambert law. However, at high incident fluence, the transmittance of the solutions decreases with increasing input fluence and a nonlinear relationship is observed between the output and input fluence, suggesting that the incorporation of conjugated azobene or stilene group into the polyacetylene structures has endowed them with

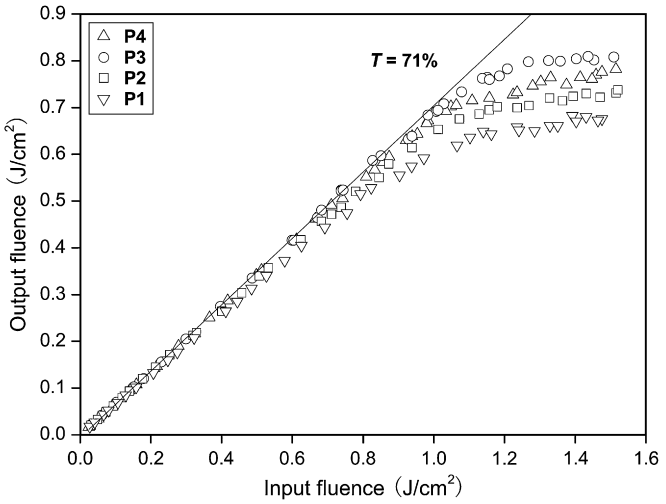

Fig. 6. Optical responses to laser light of **P1** (Table 1, no. 1), **P2** (Table 1, no. 2), **P3** (Table 1, no.3), and **P4** (Table 1, no. 10) in THF with a linear transmission of 71%.

novel optical limiting properties. With a further increase in the incident fluence, the transmitted fluence of **P1**–**P4** solutions reaches a plateau. Simultaneously, we also found that the limiting threshold (incident fluence at which the output fluence starts to deviate from linearity) and amplitude (saturated output intensity) of resultant polymers are affected by molecular structure (Table 2). As seen in Table 2, **P1** showed a little better optical limiting property than **P2** and **P3**, which is consistent with the result of the nonlinear optical property. Different from their nonlinear optical properties, polymer **P4** with C=C π-electron conjugation bridge showed better optical property than **P3** with N=N π-electron conjugation bridge although **P3** has larger $\chi^{(3)}$ than **P4**, for example, the limiting threshold and amplitude are 0.85 and 0.82 J/cm^2 for **P3** and 0.74 and 0.77 J/cm^2 for **P4** at the same transimittance, which may be originated from the weaker ground electronic absorption of **P4** than that of **P3** at 532 nm wavelength. Although **P1**–**P4** could limit the energy of harsh laser pulses, the OL properties were still inferior to those of PAs directly connected by conjugated azobenzene [4,5], which may result from the weakened electronic interactions by spacer between azobenzene and the polyacetylene main chain. Simultaneously, we measured the electron absorption spectrum of the polymer solutions before and after the laser irradiation and found that the pattern and intensity of their UV–vis absorption spectra have almost no change, hinting that the polymers possess good photostability. In contrast, the transmittance of relative parent polymer poly(PA) solution continually increases instead of decreasing due to the laser-induced photolysis of the polyacetylene chains [48]. Thus, it is evident that the incorporation of azobenzene or stilbene chromophores to the polymer structures has endowed polyacetylenes with novel optical limiting property and good photostability.

Table 2
Properties of the polymers

Polymer	Thermal stability[a] T_d (°C)	Nonlinear optical values[b]			Limiting threshold[c] (J/cm^2)	Limiting amplitude[d] (J/cm^2)
		α_2 (m/W)	n_2 (m^2/W)	$\chi^{(3)}$ (esu)		
P1	222	2.90×10^{-10}	2.78×10^{-17}	2.28×10^{-11}	0.32	0.67
P2	238	2.53×10^{-10}	2.79×10^{-17}	2.24×10^{-11}	0.41	0.71
P3	267	3.98×10^{-10}	1.49×10^{-17}	1.69×10^{-11}	0.85	0.82
P4	281	1.40×10^{-10}	–	4.69×10^{-12}	0.74	0.77

[a] Temperature for 5% weight loss.
[b] Measured by Z-scan technique with an 4 ns Nd:YAG laser system at 1 Hz repetition rate and 532 nm wavelength.
[c] Incident fluence at which the output fluence starts to deviate from linearity.
[d] Maximum output fluence.

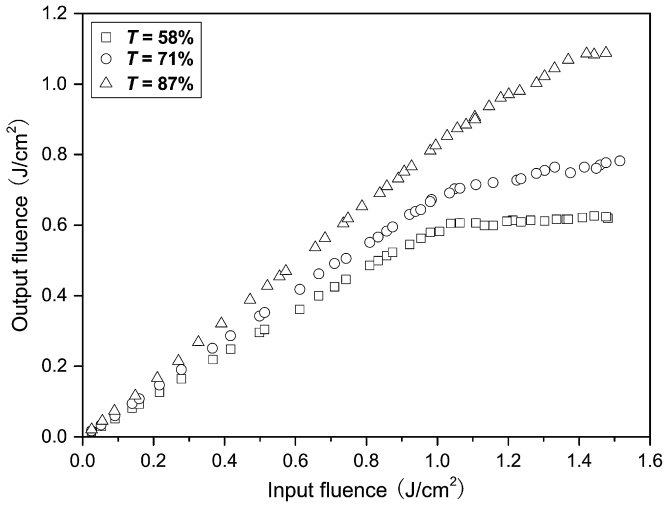

Fig. 7. Optical responses to 4 ns, 1 Hz pulses of 532 nm laser light of THF solutions of **P4** (sample taken from Table 1, No. 10) with different linear transmittances.

The NLO mechanisms for optical limiting of organic compounds can be two-photon absorption (TPA) or reverse saturable absorption (RSA). Generally, TPA can be yielded in principle under the laser irradiation of picosecond or shorter pulses. RSA can be achieved on nanosecond or longer pulses, rather than a picosecond time scale, because of the different excited-state lifetimes involved in a multilevel energy process [49]. In this work, the polymers are excited by the laser with 4 ns pulse width at 532 nm. Therefore, we consider that the optical limiting properties of the polymers may mainly originate from RSA.

The optical limiting property of RSA molecules can be evaluated by the ratio of the excited-state absorption cross-section (σ_{ex}) to the ground state absorption cross-section (σ_0) of molecules, which was defined as $\sigma_{ex}/\sigma_0 = \ln T_{sat}/\ln T_0$. T_{sat} is the saturated transmittance for high degrees of excitation [50]. The larger the value of σ_{ex}/σ_0, the better the optical limiting performance. In our experimental set up, although we are unable to reach the saturable transmittance for these compounds, we can use the transmittance at 1.5 J/cm^2 to calculate the lowest bound for σ_{ex}/σ_0. Based on the experiment data illustrated in Fig. 6, the calculated values of σ_{ex}/σ_0 for **P1**–**P4** are 2.35, 2.18, 1.76 and 1.95, respectively, further confirming that their optical limiting mechanism are mainly originated from reverse saturable absorption yielded by large excitation state absorption cross-section.

Fig. 7 shows the optical limiting performances of **P4** in THF with different concentrations. It can be found that the limiting effect was affected by concentration, with higher concentration solutions exhibiting better performances. For example, the limiting threshold of **P4** solution decreased from 0.74 to 0.66 J/cm^2 when linear transmittance decreases from 71% ($c = 0.52$ mg/mL) to 58% ($c = 0.75$ mg/mL). On the contrary, the threshold increased from 0.74 to 0.95 J/cm^2 when linear transmittance was increased from 71% to 87% ($c = 0.28$ mg/mL). Similar results were also found by Kojima et al.'s [51] and our previous publications [4,31]. It is the reason that the solution with a high concentration has more molecules per unit volume, which should absorb the energy of the harsh laser more efficiently.

4. Conclusion

In this work, we designed and synthesized a group of functional polyacetylenes substituted by different chromophore pendants with different end groups and different π-electron conjugated bridges and investigated the effects of the molecular structure on their optical properties. It is found that incorporation of azobenzene or stilbene NLO chromophore into polyacetylenes has endowed the polyacetylenes with novel optical limiting properties, large $\chi^{(3)}$ susceptibility, and good thermal and photostability. Functional polyacetylene with stilbene chromophore pendant shows better optical limiting property than that with azobenzene chromophore pendant. Their optical limiting mechanisms are mainly originated from reverse saturable absorption. Their nonlinear optical properties are significantly affected by their molecular structure and the longer spacer group will decrease the electronic interaction between chromophore pendant and conjugation backbone of polyacetylene to result in low nonlinear optical properties.

Acknowledgement

This research was financially supported by the National Natural Science Fund of China (Grant Nos. 90606011 and 50472038), Program for New Century Excellent Talents in University (NCET-04-0588), and Ph.D. Program Foundation of Ministry of Education of China (No. 20070255012).

Reference

[1] Tutt LW, Kost A. Nature 1992;356:225–6.
[2] Spangler CW. J Mater Chem 1999;9:2013–20.
[3] Tutt LW, Boggess TF. Prog Quantum Electron 1993;17:299–338.
[4] Yin S, Xu H, Shi W, Gao Y, Song Y, Lam JWY, et al. Polymer 2005;46:7670–7.
[5] Yin S, Xu H, Fang M, Shi W, Gao Y, Song Y. Macromol Chem Phys 2005;206:1549–57.
[6] Zhang H, Zelmon DE, Deng L, Liu HK, Teo BK. J Am Chem Soc 2001;123:11300–1.
[7] Vestberg R, Westlund R, Eriksson A, Lopes C, Carlsson M, Eliasson B, et al. Macromolecules 2006;39:2238–46.
[8] Kajzar F, Etemad S, Baker GL, Messier J. Solid State Commun 1987;63:1113–7.
[9] Fann WS, Benson S, Madey JMJ, Etemad S, Baker GL, Kajzar F. Phys Rev Lett 1989;62:1492–5.
[10] Takahashi A. Synth Met 1997;85:1087–8.
[11] Geng J, Zhao X, Zhou E, Li G, Lam JWY, Tang BZ. Polymer 2003;44:8095–102.
[12] Ting C-H, Chen J-T, Hsu C-S. Macromolecules 2002;35:1180–9.
[13] Schenning APHJ, Fransen M, Meijer EW. Macromol Rapid Commun 2002;23:265–70.
[14] Okoshi K, Sakajiri K, Kumaki J, Yashima E. Macromolecules 2005;38:4061–4.
[15] Sanda F, Nakai T, Kobayashi N, Masuda T. Macromolecules 2004;37:2703–8.
[16] Law CCW, Lam JWY, Qin A, Dong Y, Kwok HS, Tang BZ. Polymer 2006;47:6642–51.
[17] Qu J, Suzuki Y, Shiotsuki M, Sanda F, Masuda T. Polymer 2007;48:4628–36.
[18] Qu J, Kawasaki R, Shiotsuki M, Sanda F, Masuda T. Polymer 2006;47:6551–9.
[19] Lam JWY, Dong Y, Kwok HS, Tang BZ. Macromolecules 2006;39:6997–7003.
[20] Qu J, Suzuki Y, Shiotsuki M, Sanda F, Masuda T. Polymer 2007;48:6491–500.
[21] Maeda K, Morino K, Okamoto Y, Sato T, Yashima E. J Am Chem Soc 2004;126:4329–42.
[22] Tang BZ, Chen HZ, Xu RS, Lam JWY, Cheuk KKL, Wong HNC, et al. Chem Mater 2000;12:213–21.
[23] Kanaya T, Tsukushi I, Kaji K, Sakaguchi T, Kwak G, Masuda T. Macromolecules 2002;35:5559–64.
[24] Raharjo RD, Lee HJ, Freeman BD, Sakaguchi T, Masuda T. Polymer 2005;46:6316–24.
[25] Suzuki Y, Shiotsuki M, Sanda F, Masuda T. Macromolecules 2007;40:1864–7.
[26] Zhan X, Yang M, Xu G, Liu X, Ye P. Macromol Rapid Commun 2001;22:358–62.
[27] Zhan X, Yang M, Lei Z, Li Y, Liu Y, Yu G, et al. Adv Mater 2001;12:51–3.
[28] Zeng Q, Li Z, Li Z, Ye C, Qin J, Tang BZ. Macromolecules 2007;40:5634–7.
[29] Li Z, Li Q, Qin A, Dong Y, Lam JWY, Dong Y, et al. J Polym Sci Part A Polym Chem 2006;44:5672–81.
[30] Sata T, Nomura R, Wada T, Sasabe H, Masuda T. J Polym Sci Part A Polym Chem 1998;36:2489–92.
[31] Yin S, Xu H, Su X, Gao Y, Song Y, Lam JWY, et al. Polymer 2005;46:10592–600.
[32] Xu H, Yin S, Zhu W, Song Y, Tang B. Polymer 2006;47:6986–92.
[33] Yin S, Xu H, Su X, Li G, Song Y, Lam JWY, et al. J Polym Sci Part A Polym Chem 2006;44:2346–57.
[34] Qu S, Song Y, Du C, Wang Y, Gao Y, Liu S, et al. Opt Commun 2001;196:317–23.
[35] Sheik-Bahae M, Said AA, Wei T-H, Hagan DJ, Stryland EWV. IEEE J Quantum Electron 1990;26:760–9.
[36] Hwang J-J, Lin R-L, Shieh R-L, Jwo J-J. J Mol Catal A Chem 1999;142:125–39.
[37] Teraguchi M, Masuda T. Macromolecules 2000;33:240–2.
[38] Yin S, Xu H, Shi W, Gao Y, Song Y, Tang BZ. Dyes Pigments 2006;71:138–44.
[39] Masuda T, Tang BZ, Higashimura T, Yamaoka H. Macromolecules 1985;18:2369–73.

[40] Lam JWY, Dong Y, Cheuk KKL, Luo J, Xie Z, Kwok HS, et al. Macromolecules 2002;35:1229–40.
[41] Tang BZ, Kong X, Wan X, Peng H, Lam WY, Feng XD, et al. Macromolecules 1998;31:2419–32.
[42] Li Z, Dong Y, Haussler M, Lam JWY, Dong Y, Wu L, et al. J Phys Chem B 2006; 110:2302–9.
[43] Hua JL, Lam JWY, Dong H, Wu L, Wong KS, Tang BZ. Polymer 2006;47: 18–22.
[44] Falconieri M, D'Amato R, Furlani A, Russo MV. Synth Met 2001;124:217–9.
[45] Neher D, Kaltbeitzel A, Wolf A, Bubeck C, Wegner G. J Phys D Appl Phys 1991; 24:1193–202.
[46] Yin S, Xu H, Su X, Wu L, Song Y, Tang BZ. Dyes Pigments 2007;75:675–80.
[47] Guang S, Yin S, Xu H, Zhu W, Gao Y, Song Y. Dyes Pigment 2007;73:285–91.
[48] Tang BZ, Xu H. Macromolecules 1999;32:2569–76.
[49] Sun WF, Bader MM, Carvalho T. Opt Commun 2003;215:185–90.
[50] Perry JW, Mansour K, Marder SR, Perry KJ, Daniel Alvarez J, Choong I. Opt Lett 1994;19:625–7.
[51] Kojima Y, Matsuoka T, Sato N, Takahashi H. Macromolecules 1995;28:2893–6.